Identification of novel immune and barrier genes in atopic dermatitis by means of laser capture microdissection

Hitokazu Esaki, MD,[a,b]* David A. Ewald, MSc,[a,c,d]* Benjamin Ungar, BA,[a,b] Mariya Rozenblit, BA,[a,b] Xiuzhong Zheng, MSc,[a] Hui Xu, MSc,[a] Yeriel D. Estrada, BS,[a,b] Xiangyu Peng, MSc,[a,b] Hiroshi Mitsui, MD, PhD,[a] Thomas Litman, PhD,[c] Mayte Suárez-Fariñas, PhD,[a] James G. Krueger, MD, PhD,[a] and Emma Guttman-Yassky, MD, PhD[a,b] *New York, NY, and Ballerup and Lyngby, Denmark*

Background: The molecular signature of atopic dermatitis (AD) lesions is associated with T_H2 and T_H22 activation and epidermal alterations. However, the epidermal and dermal AD transcriptomes and their respective contributions to abnormalities in respective immune and barrier phenotypes are unknown.
Objective: We sought to establish the genomic profile of the epidermal and dermal compartments of lesional and nonlesional AD skin compared with normal skin.
Methods: Laser capture microdissection was performed to separate the epidermis and dermis of lesional and nonlesional skin from patients with AD and normal skin from healthy volunteers, followed by gene expression (microarrays and real-time PCR) and immunostaining studies.
Results: Our study identified novel immune and barrier genes, including the IL-34 cytokine and claudins 4 and 8, and showed increased detection of key AD genes usually undetectable on arrays (ie, *IL22*, thymic stromal lymphopoietin *[TSLP]*, *CCL22*, and *CCL26*). Overall, the combined epidermal and dermal transcriptomes enlarged the AD transcriptome, adding 674 upregulated and 405 downregulated differentially expressed genes between lesional and nonlesional skin to the AD transcriptome. We were also able to localize individual transcripts as primarily epidermal (defensin, beta 4A *[DEFB4A]*) or dermal (*IL22*, cytotoxic T-lymphocyte antigen 4 *[CTLA4]*, and *CCR7*) and link their expressions to possible cellular sources.
Conclusions: This is the first report that establishes robust epidermal and dermal genomic signatures of lesional and nonlesional AD skin and normal skin compared with whole tissues. These data establish the utility of laser capture microdissection to separate different compartments and cellular subsets in patients with AD, allowing localization of key barrier or immune molecules and enabling detection of gene products usually not detected on arrays. (J Allergy Clin Immunol 2015;135:153-63.)

Key words: *Atopic dermatitis, laser capture microdissection, IL-34, claudins 8 and 4, immune, barrier*

Atopic dermatitis (AD) is the most common inflammatory skin disease.[1,2] Although its pathogenesis is not fully understood, both barrier and immune components have been suggested to play key roles in AD, as indicated by the "outside-in" and "inside-out" hypotheses.[3-10] Whereas barrier-related molecules are largely epidermal, inflammatory responses are derived from both the epidermal (ie, keratinocytes and Langerhans cells [LCs]) and dermal (ie, T cells and dendritic cells [DCs]) compartments.

Using genomic analyses on whole tissue/bulk samples, we have previously shown that the AD phenotype/transcriptome is associated with polar immune activation of T_H2/T_H22, as well as T_H1 and T_H17, pathways and corresponding epidermal alterations (epidermal hyperplasia and abnormal differentiation).[11-14] However, bulk sample genomic analysis (by using microarrays and real-time PCR [RT-PCR]) presents some limitations. First, it is difficult to determine whether altered gene expression is due to expansion (hypertrophy) of one tissue compartment versus altered gene expression at the cellular level. Second, it cannot localize a particular gene/transcript to an epidermal/dermal compartment. Finally, low-abundance genes are often present at less than the detection level of conventional microarrays because of dilution of mRNA within full-thickness samples with more dominant products.

Laser capture microdissection (LCM) is an established technique for procuring subpopulations of tissues/cells of interest

From [a]the Laboratory for Investigative Dermatology, Rockefeller University, New York; [b]the Department of Dermatology, Icahn School of Medicine at Mount Sinai, New York; [c]Molecular Biomedicine, LEO Pharma, Ballerup; and [d]the Center for Microbial Biotechnology, DTU Systems Biology, Technical University of Denmark, Lyngby.
*These authors contributed equally to this work.
J.G.K. and M.S.-F. were supported by grant 5UL1RR024143-02 from the National Center for Research Resources (NCRR), a component of the National Institutes of Health (NIH), and the NIH Roadmap for Medical Research. Supported in part by grant no. UL1TR000043 from the National Center for Advancing Translational Sciences (NCATS, NIH Clinical and Translational Science Award [CTSA]) program. E.G.-Y. was supported by the Dermatology Foundation Physician Scientist Career Development Award and by Leo Pharma, and D.A.E. is a joint PhD student of Leo Pharma and DTU and partly funded by the Danish Ministry of Higher Education and Science.
Disclosure of potential conflict of interest: D. A. Ewald is employed by LEO Pharma and has received or has grants pending from the Danish Ministry of Higher Education and Science. T. Litman is an employee of LEO Pharma. J. G. Krueger and his institution have received funding from Novartis, Pfizer, Amgen, Lilly, Merck, Kadmon, Dermira, Boehringer, Innovaderm, Kyowa, BMS, Serono, Janssen, Delenex, AbbVie, Sanofi, Baxter, Paraxel, Xenoport, and Kineta. E. Guttman-Yassky receives compensation for board membership from Sanofi Aventis, Regeneron, Stiefel/GlaxoSmithKline, Medimmune, Celgene, Anacor, and LEO Pharma; receives consultancy fees from Regeneron, Sanofi Aventis, Medimmune, Celgene, Steifel/GlaxoSmithKline, Celsus, BMS, Amgen, and Drais; and has received or has grants pending from Regeneron, Celgene, BMS, and Janssen. The authors declare that they have no other relevant conflicts of interest.
Received for publication September 19, 2014; revised October 28, 2014; accepted for publication October 30, 2014.
Corresponding author: Emma Guttman-Yassky, MD, PhD, Department of Dermatology, Icahn School of Medicine at Mount Sinai Medical Center, 5 E 98th St, New York, NY 10029. E-mail: Emma.Guttman@mountsinai.org.
0091-6749/$36.00
© 2014 American Academy of Allergy, Asthma & Immunology
http://dx.doi.org/10.1016/j.jaci.2014.10.037

Abbreviations used

AD: Atopic dermatitis
CE: Cornified envelope
CLDN: Claudin
CSF-1R: Colony-stimulating factor 1 receptor
CTLA4: Cytotoxic T-lymphocyte antigen 4
DC: Dendritic cell
DEFB4A: Defensin, beta 4A
DEG: Differentially expressed gene
EDC: Epidermal differentiation complex
FCH: Fold change
FDR: False discovery rate
FLG: Filaggrin
GZMB: Granzyme B
ICOS: Inducible T-cell costimulator
LC: Langerhans cell
LCM: Laser capture microdissection
LOR: Loricrin
MX1: Myxovirus (influenza virus) resistance 1, interferon-inducible protein p78 (mouse)
PI3: Peptidase inhibitor 3, skin-derived
RT-PCR: Real-time PCR
SPRR: Small proline-rich protein
TJ: Tight junction

under direct microscopic visualization to study alterations in disease states.[15] Our group has previously demonstrated that epidermal and dermal separation of lesional and nonlesional samples from patients with psoriasis and normal samples by using LCM complemented by microarrays largely increases the detection of low-abundance genes compared with whole-tissue analyses.[16,17] Despite the pathogenic relevance of separating the epidermal and dermal compartments, such studies are unavailable in patients with AD.

In this study we sought to determine the molecular phenotypes of the epidermal and dermal compartments of lesional and nonlesional AD skin (compared with skin from healthy subjects). Overall, our results (1) enlarged the AD transcriptome; (2) detected low-abundance genes (which are usually present at less than detection levels on whole-tissue microarrays [eg, *IL22* and thymic stromal lymphopoietin *[TSLP]*); and (3) identified novel immune and barrier genes (ie, *IL34*, claudin 4 *[CLDN4]*, and *CLDN8*) and suggested possible cellular sources of immune markers (ie, CCR7).

METHODS

Skin samples

Paired nonlesional and lesional AD skin biopsy specimens were collected from 5 patients with moderate-to-severe chronic AD (3 male and 2 female patients; age, 27-59 years; mean age, 39.4 years; see Table E1 in this article's Online Repository at www.jacionline.org) under institutional review board–approved protocols. Normal skin samples from healthy volunteers (n = 10) that had been collected for a prior LCM publication[18] were also included. Paired epidermal, dermal, and full-thickness lesional and nonlesional samples were used for RT-PCR and microarray analysis (n = 5 in each group). Lesional and nonlesional expression values were compared with 10 epidermal, 6 dermal, and 6 bulk corresponding normal samples. For RT-PCR confirmation, 3 normal paired epidermal and dermal samples were used because of the limited available mRNA.

Slide preparation and LCM

LCM was performed according to the manufacturer's protocol for the CellCut system (Molecular Machines & Industries, Haslett, Mich; see the Methods section in this article's Online Repository at www.jacionline.org).

RNA extraction

Total RNA was extracted with the RNeasy Micro Kit (Qiagen, Valencia, Calif), according to the manufacturer's protocol, with on-column DNase digestion.

Sample preparation for gene chip analysis

Target amplification and labeling was performed according to the Affymetrix protocols for 2-cycle cDNA synthesis by using Affymetrix Human Genome U133 Plus 2.0 arrays (Affymetrix, Santa Clara, Calif), as previously reported.[16]

Sample preparation for quantitative RT-PCR

Reverse transcription to cDNA from RNA of LCM samples was carried out by using the High Capacity cDNA Reverse Transcription kit (Applied Biosystems, Foster City, Calif), cDNA was amplified with TaqMan PreAmp Master Mix (Applied Biosystems), and the preamplified cDNA product was analyzed with TaqMan Gene Expression Master Mix, according to the manufacturer's instructions. The RT-PCRs for each assay were run in triplicate, and all data were normalized to human acidic ribosomal protein P0. The primers and probes used in this study are listed in Table E2 in this article's Online Repository at www.jacionline.org.

Immunohistochemistry and immunofluorescence

Immunohistochemistry and immunofluorescence were performed on frozen skin sections, as previously described.[19] The antibodies used in this study are listed in Table E3 in this article's Online Repository at www.jacionline.org.

Statistical analysis

Preprocessing and statistical analysis of microarray data were conducted with R (R-project.org) and Bioconductor software packages.[20] Full details of the pipeline and downstream analysis are described in the Methods section in this article's Online Repository. Succinctly, the Harshlight package[21] was used to quality control the images, and expression values were obtained by using the GCRMA algorithm.[22] Batch adjustments were carried out with the ComBat algorithm, and mixed-effect models in the limma package were used to model differential expression.[23-25] Genes with a false discovery rate (FDR) of less than 0.05 and a fold change of greater than 2 were considered significantly differentially expressed. Similar models were used to analyze $\log_2$-transformed values of normalized RT-PCR data.

RESULTS

LCM localizes genes selectively expressed in the dermis and epidermis

We performed LCM to collect epidermal and dermal (papillary, reticular, and inflammatory aggregate) cells in frozen sections of lesional, nonlesional, and normal skin samples, as shown in Fig 1, *A*. Microarray profiling of lesional, nonlesional, and normal epidermal and dermal tissues was performed with Affymetrix HGU133Plus2.0 microarrays to define the epidermal and dermal transcriptomes. A heat map of epidermis- and dermis-specific genes shows clear separation of differentially expressed genes (DEGs) localized to the epidermis and dermis across lesional, nonlesional, and normal samples (see Fig E1 in this article's

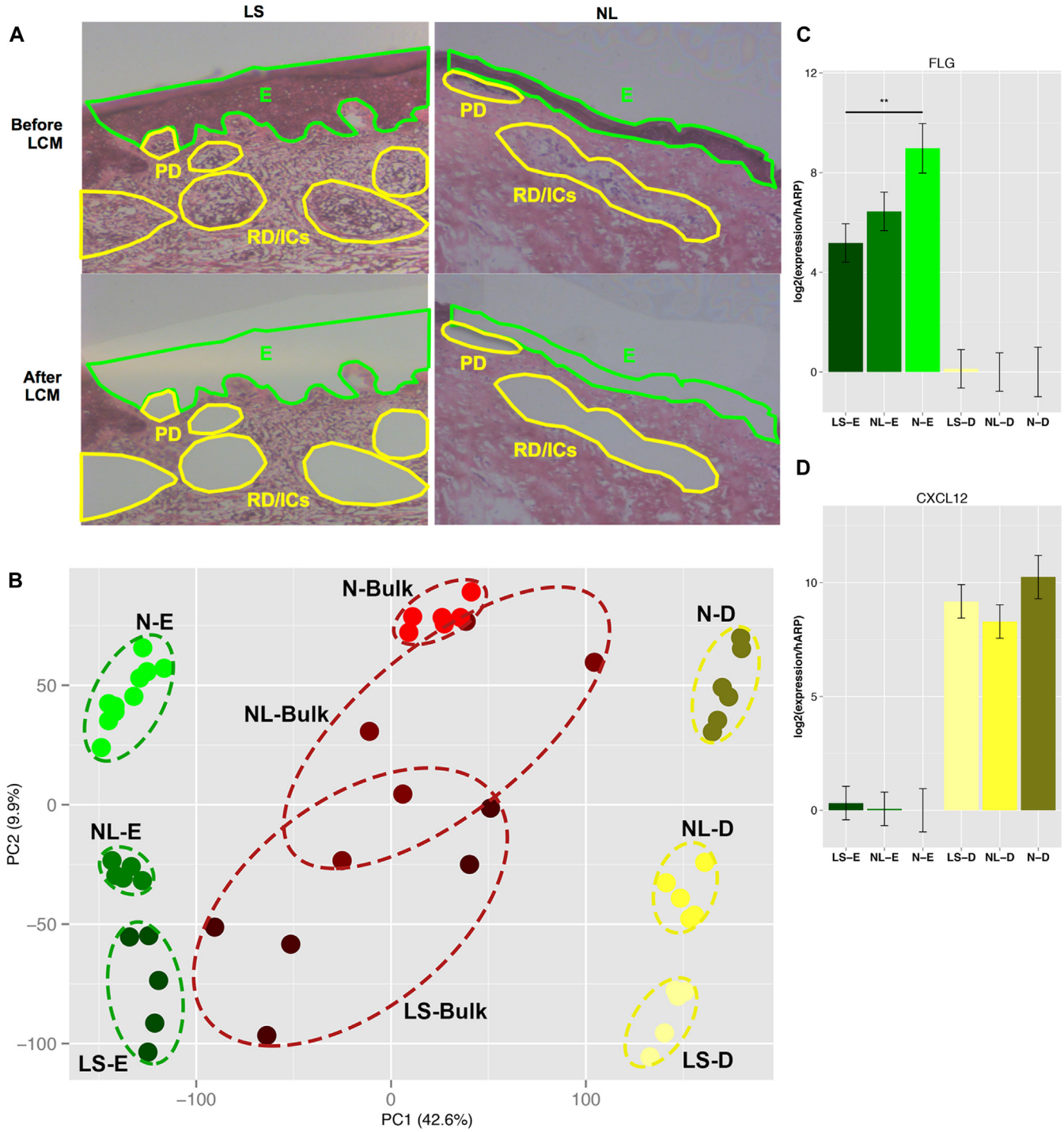

FIG 1. A, Representative hematoxylin and eosin staining of lesional *(LS)* and nonlesional *(NL)* AD skin. LCM was performed in the indicated zones (*green*: epidermis *[E]*; *yellow*: papillary dermis *[PD]*, reticular dermis *[RD]*, and inflammatory aggregates *[ICs]*). **B,** Principal component *[PC]* analysis plot showing clear separation of groups. **C** and **D,** mRNA expression of *FLG* (Fig 1, *C*) and *CXCL12* (Fig 1, *D*) in the epidermis *(E)* and dermis *(D)* of lesional *(LS)* and nonlesional *(NL)* AD and normal *(N)* skin. Values are presented as means ± SDs. $^{**}P < .01$.

Online Repository at www.jacionline.org). A principal component analysis of expression values illustrates the lack of outliers and that samples cluster in accordance with tissue type (Fig 1, *B*). Markers primarily considered dermal (*CXCL12*, *CD93*, and collagens [*COL1A2* and *COL6A3*]) were highly represented in the dermis (see Tables E4, *A*, and E5, *A*, in this article's Online Repository at www.jacionline.org), and epidermal markers (filaggrin [FLG], loricrin [LOR], late cornified envelope [LCE], and small proline-rich proteins [SPRRs]) were localized to the epidermis, which is consistent with the clear

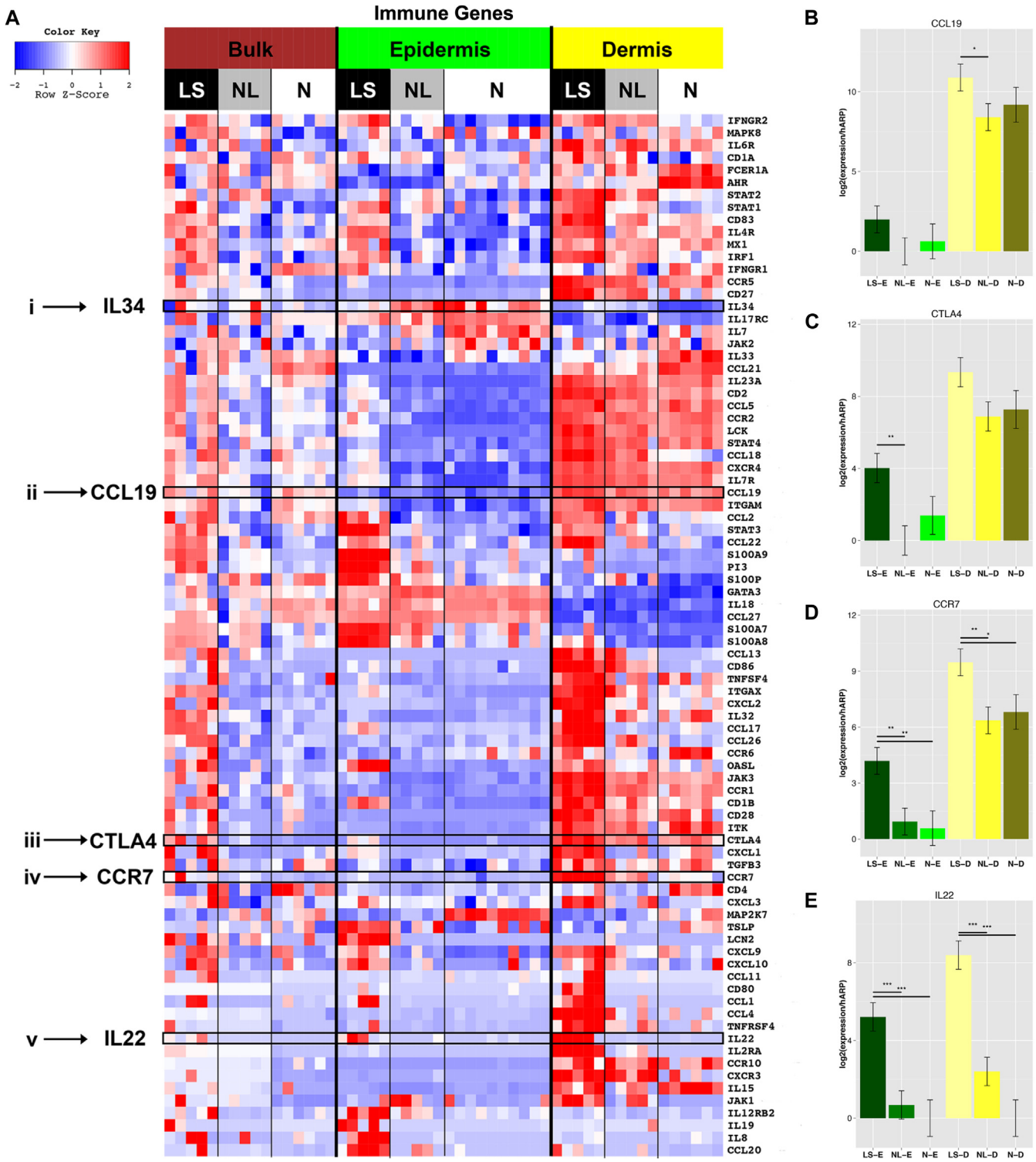

FIG 2. A, Heat map of immune-related genes organized by compartment. FCHs comparing lesional *(LS)*, nonlesional *(NL)*, and normal *(N)* skin in bulk samples *(B)* and the epidermis *(E)* dermis *(D)* are shown (n = 5 AD specimens and n = 6, 10, and 6 normal bulk, epidermal, dermal specimens, respectively). **B-E,** mRNA expression, as determined by using RT-PCR, of *CCL19* (Fig 2, *B*), *CTLA4* (Fig 2, *C*), *CCR7* (Fig 2, *D*), and *IL22* (Fig 2, *E*) in the epidermis *(E)* and dermis *(D)* of lesional *(LS)* and nonlesional *(NL)* AD skin and normal *(N)* skin. Values are presented as means ± SDs in Fig 2, *B* through *E*. $*P < .05$, $**P < .01$, and $***P < .001$.

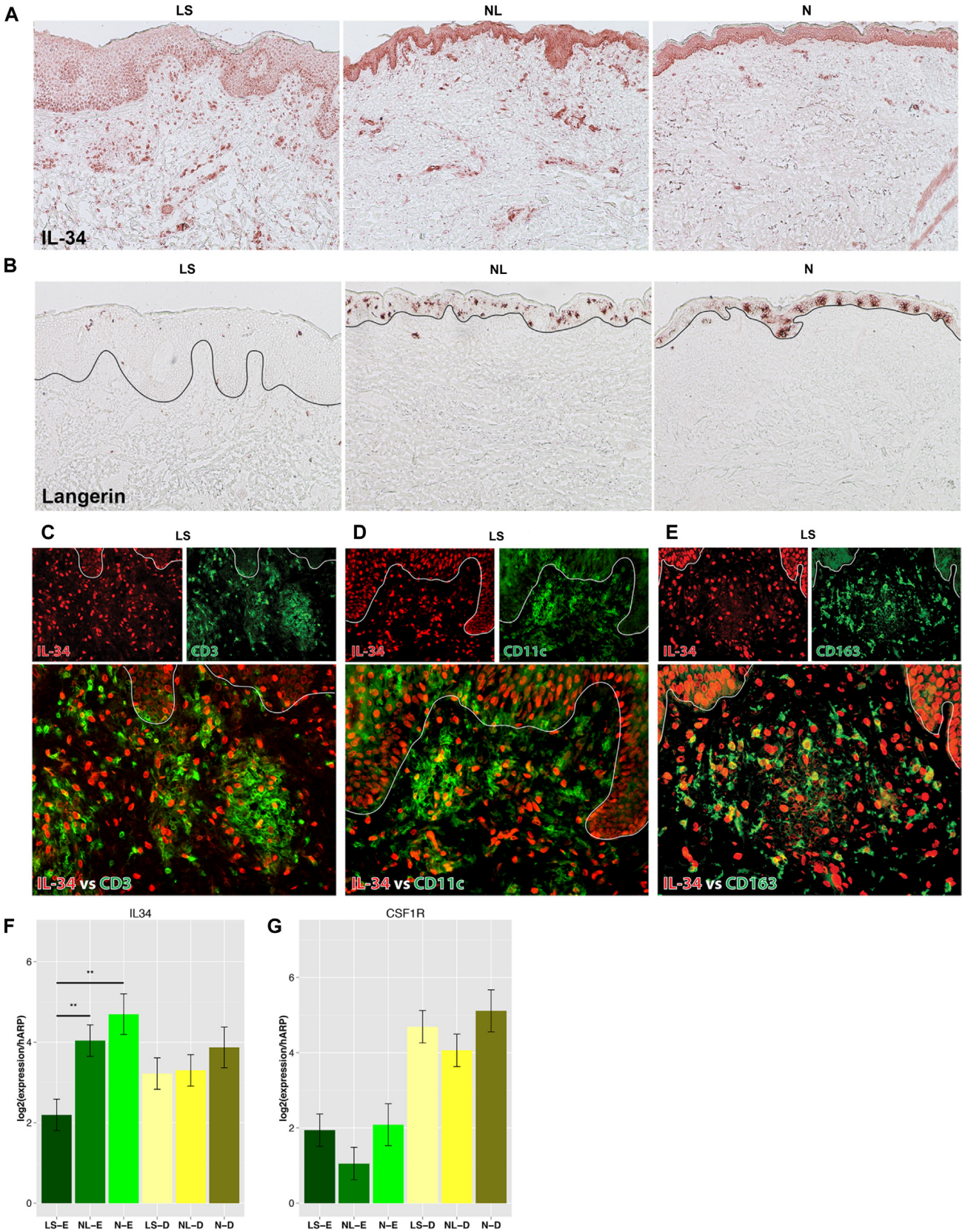

FIG 3. A and **B,** Representative staining of IL-34 (Fig 3, *A*) and langerin (Fig 3, *B*) in lesional *(LS)* and nonlesional *(NL)* AD and normal *(N)* skin. **C-E,** Representative double immunofluorescence for coexpression of IL-34 *(red)* versus CD3 (*green*; Fig 3, *C*), CD11c (*green*; Fig 3, *D*), and CD163 (*green*; Fig 3, *E*) in lesional *(LS)* skin. **F** and **G,** mRNA expression of *IL34* (Fig 3, *F*) and its receptor, *CSF1R* (Fig 3, *G*), in the epidermis *(E)* and dermis *(D)* of lesional *(LS)*, nonlesional *(NL)*, and normal *(N)* skin. Values are presented as means ± SDs. $^{**}P < .01$.

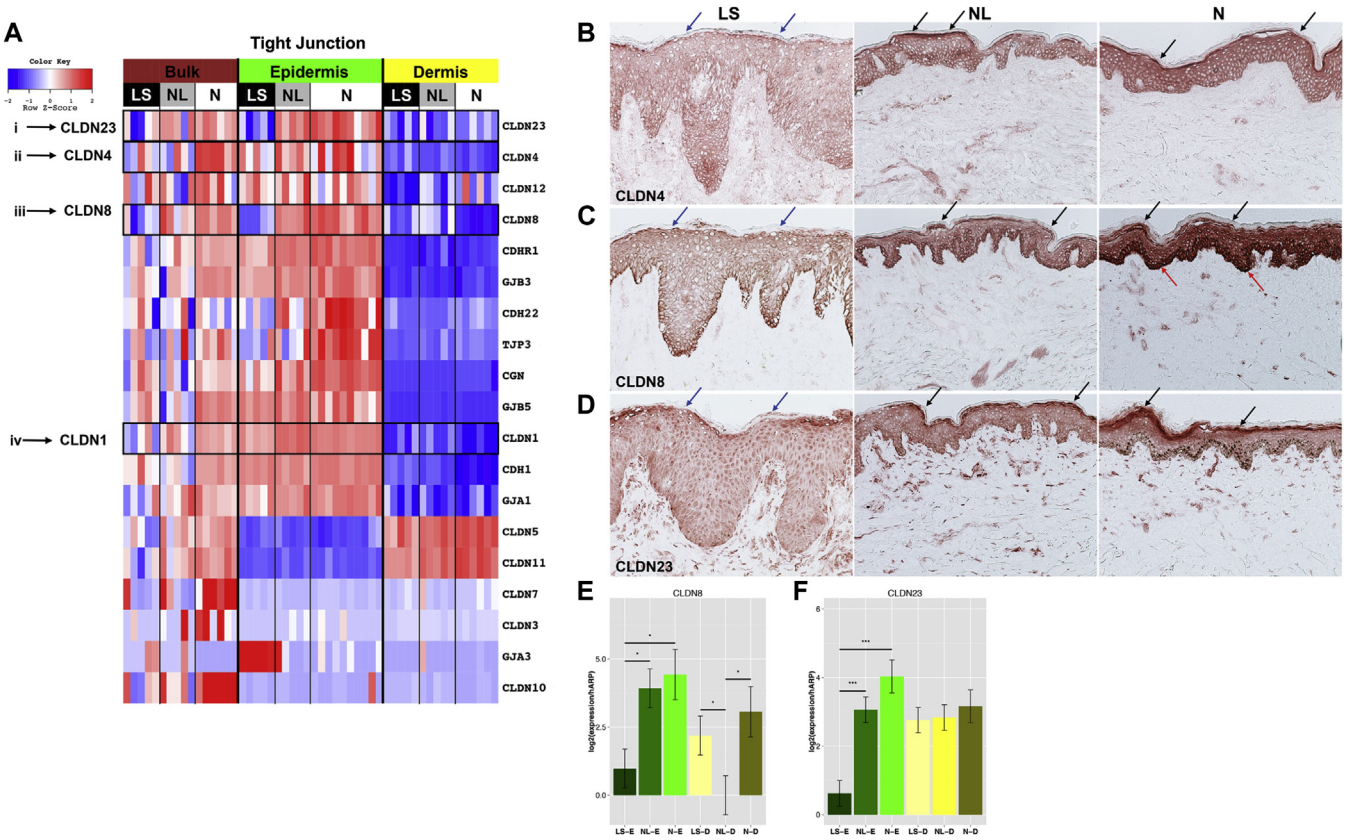

FIG 4. A, Heat map of barrier-related gene FCHs comparing lesional *(LS)*, nonlesional *(NL)*, and normal *(N)* skin in bulk, epidermal, and dermal specimens (n = 5 AD specimens and n = 6, 10, and 6 normal bulk, epidermis, and dermis specimens, respectively). **B-D,** Representative CLDN4 (Fig 4, *B*), CLDN8 (Fig 4, *C*), and CLDN23 (Fig 4, *D*) staining in lesional *(LS)*, nonlesional *(NL)*, and normal *(N)* skin. *Arrows*, Increased stratum corneum *(black)*, decreased lesional stratum corneum *(blue)*, and increased normal skin basal layer *(red)* staining. **E** and **F,** Expression of *CLDN8* (Fig 4, *E*) and *CLDN23* (Fig 4, *F*) in the epidermis *(E)* and dermis *(D)* of lesional *(LS)*, nonlesional *(NL)*, and normal *(N)* skin. Values are presented as means ± SDs. $^{*}P < .05$ and $^{***}P < .001$.

epidermal-dermal separation (see Tables E4, *B*, and E5, *B*). The accuracy of the LCM separation was validated by using RT-PCR, with greater than 69.7-fold and greater than 846.2-fold enrichment of the mRNA expressions of *FLG* and *CXCL12* in the epidermis versus dermis, respectively, in normal tissues (Fig 1, *C* and *D*).

LCM enlarges the AD transcriptome and increases detection of low-abundance immune genes on microarrays

To characterize the AD phenotype within each compartment, we defined the lesional epidermal and dermal transcriptomes as the set of DEGs between lesional and nonlesional tissue within each compartment, respectively, by using the classical criteria of an FCH of greater than 2.0 and an FDR of less than 0.05. Combining the epidermal and dermal transcriptomes, many more compartment-specific DEGs were identified (860 upregulated and 495 downregulated, see Fig E2 in this article's Online Repository at www.jacionline.org), adding 674 upregulated and 405 downregulated DEGs to the recently defined AD transcriptome.[11,12,26] The bulk transcriptome consists of 710 upregulated and 487 downregulated DEGs, whereas the LCM epidermal transcriptome contains 566 upregulated and 268 downregulated DEGs, and the LCM dermal transcriptome contains 330 upregulated and 244 downregulated DEGs. Little overlap was observed between the epidermal and dermal transcriptomes (only 36 upregulated and 17 downregulated DEGs were detected in both).

Overall, the top 25 upregulated and downregulated genes in each of the epidermal and dermal lesional transcriptomes included many genes that have been shown to contribute to the AD phenotype (see Tables E6 and E7 in this article's Online Repository at www.jacionline.org).[11,12] The top 25 upregulated genes in the lesional epidermal transcriptome consisted of proliferation-related (*KRT6A*, *KRT6B*, and *KRT16*), epidermal differentiation complex (EDC; S100 genes), inflammatory (matrix metalloproteinase 12 *[MMP12]*), and antimicrobial peptide–derived (defensin, beta 4A *[DEFB4A]* and peptidase inhibitor 3, skin-derived *[PI3]*/Elafin) genes (see Table E6, *A*). The top 25 upregulated genes in the lesional dermal transcriptome included T-cell activation (granzyme B *[GZMB]* and IL-2 receptor α *[IL2RA]*), T_H2-related (*CCL17*, *CCL22*, and *CCL26*), T_H22/T_H17-related (*IL22*, *S100A8*, *CXCL1*, and *CXCL2*), and collagen (*COL6A6*, *COL6A5*, and *COL4A3*) genes (see Table E6, *B*). *IL22* expression was significantly increased in the lesional dermal transcriptome (12.46 FCHs and FDR < 0.001), whereas it was present

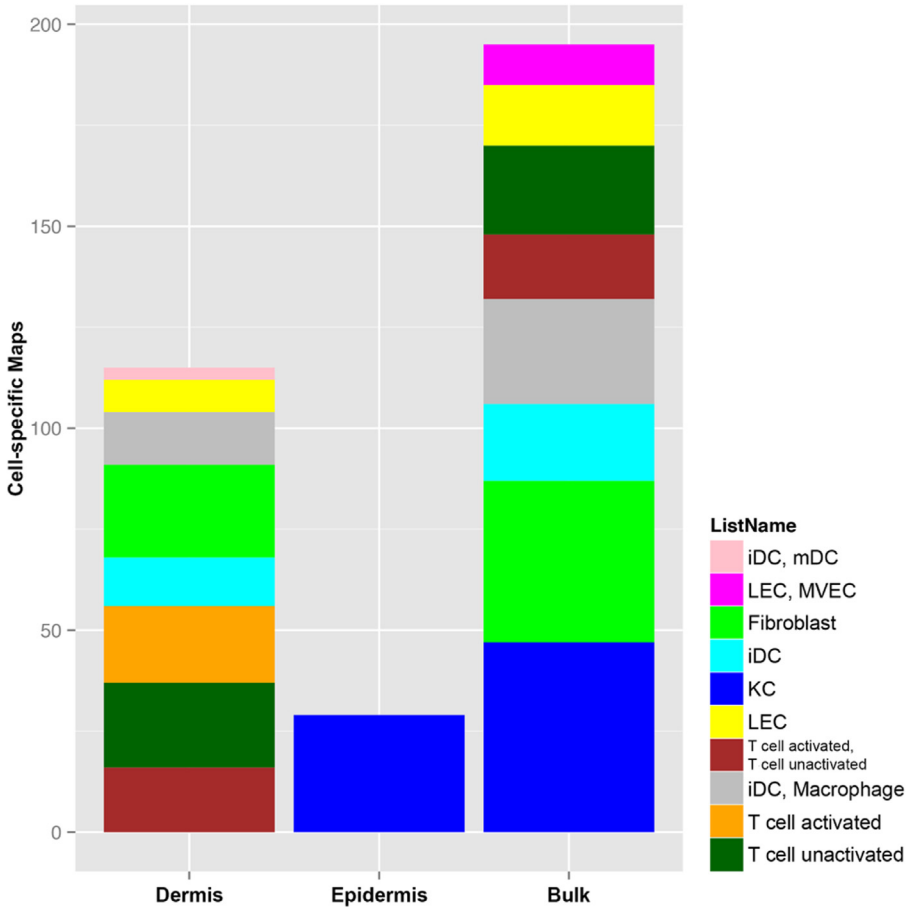

FIG 5. The cell-specific map of the LCM epidermal and dermal transcriptomes and bulk transcriptome. The cellular source of the epidermal transcriptome was mainly keratinocytes, whereas activated T cells were only significantly enriched in the LCM dermal transcriptome. *iDC,* Immature dendritic cell; *KC,* keratinocyte; *LEC,* lymphatic endothelial cell; *mDC,* mature dendritic cell; *MVEC,* microvascular endothelial cell.

at less than detection levels in previous reports,[11,12,26] indicating that LCM is a useful method to increase the sensitivity of detecting low-abundance genes.

Key inflammatory and barrier genes were uniquely detected in the LCM epidermal (see Table E8, *A*, in this article's Online Repository at www.jacionline.org) and dermal (see Table E8, *B*) transcriptomes. The unique lesional epidermal transcriptome included IL-17–related (*DEFB4A* and *CCL20*) and inflammatory (*CXCR4*, signal transducer and activator of transcription 3 *[STAT3]*, and *IL8*) genes (see Table E8, *A*). Key T_H2 (*CCL17*, *CCL22*, and *CCL26*) and T_H22 *(IL22)* markers and T-cell migration/activation markers (*CCR7* and inducible T-cell costimulator *[ICOS]*) were found within the unique lesional dermal transcriptome (see Table E8, *B*). Although the LCM approach detected an appreciably larger number of genes within bulk tissues, there was a subset of DEGs that were not identified in the corresponding epidermal and dermal transcriptomes (429 upregulated and 381 downregulated genes; Fig 2 and see Table E8, *C*). A deeper analysis of these data suggests that most of this discrepancy is created by increased or decreased gene abundance because of differing contributions of the epidermis and dermis in lesional versus nonlesional skin (see the Results section and Fig E3 in this article's Online Repository at www.jacionline.org).

We further explored the compartmental distribution of immune DEGs in lesional, nonlesional, and normal skin using our previously curated and reported immune gene subset,[19,26,27] as shown in a heat map (Fig 2, *A*, and see Table E9 in this article's Online Repository at www.jacionline.org). Among significantly upregulated genes in the lesional dermal transcriptome were T-cell (cytotoxic T-lymphocyte antigen 4 *[CTLA4]* and *CD28*), DC (integrin αX, complement component 3 receptor 4 subunit *[ITGAX]*/CD11c and *CD1A*), lymphoid-organizing chemokine (*CCR7* and its ligands [*CCL19* and *CCL21*]), and T_H2-related (*CCL11*, *CCL13*, *CCL17*, *CCL22*, *CCL26*, TNF receptor superfamily, member 4 [*TNFRSF4*/OX40], and *IL4R*) genes. Significant increases in T_H2-related *(IL7R)*, T_H17-related (*PI3*, lipocalin 2 *[LCN2]*, *CCL20*, and *STAT3*), T_H22/T_H17-related (*IL22*, *S100A8*, and *S100A9*), and T_H1-related (2′-5′-oligoadenylate synthetase-like *[OASL]*, myxovirus [influenza virus] resistance 1, interferon-inducible protein p78 [mouse] *[MX1]*, *IL12RB2*, IFN-γ receptor 2 *[IFNGR2]*, and interferon regulatory factor 1 *[IRF1]*) products were found. Using RT-PCR, we validated the primarily dermal mRNA expression of selected markers, including *IL22*, *CTLA4*, *CCR7*, and *CCL19*. High *IL22* mRNA levels were characteristic of only lesional skin (Fig 2, *B-E*). A list of DEGs in all comparisons is presented in Table E8.

IL-34: A novel cytokine identified by means of LCM

IL-34 was significantly downregulated in lesional compared with both nonlesional and normal epidermis (Fig 2, *A*, and see Table E9). IL-34 is a recently identified cytokine in mice and normal human skin[28] and is suggested to regulate LC differentiation in steady states. It has been identified as an alternative ligand to the colony-stimulating factor 1 receptor (CSF-1R), which has been shown to be expressed in epidermal LCs, dermal monocytes, and DCs.[29] IL-34 has not been previously reported in human skin diseases. We performed immunohistochemical staining of IL-34, which showed stronger epidermal staining in normal and nonlesional skin compared with lesional skin and stronger dermal staining in lesional skin (Fig 3, *A*).

Because IL-34 was reported to induce LC differentiation only in steady states,[29] langerin (CD207) staining for LCs was performed. Many fewer LCs were detected in lesional compared with both nonlesional and normal skin (Fig 3, *B*). To identify the cellular distribution of IL-34 expression in the dermis, we performed double immunofluorescence for IL-34 (red) with $CD3^+$/T cells (green; see Fig E4, *A*, in this article's Online Repository at www.jacionline.org), $CD11c^+$/DCs (green; see Fig E4, *B*), and $CD163^+$/macrophages (green; see Fig E4, *C*) in normal, nonlesional, and lesional skin. Few double-positive IL-34^+/$CD3^+$ cells were found. Many IL-34^+ cells colocalized with $CD11c^+$ and $CD163^+$ cells (Fig 3, *C-E*). Thus IL-34 in the dermis is preferentially expressed by myeloid DCs and macrophages.

We validated the lower expression of IL-34 in lesional epidermis using RT-PCR, with significantly lower *IL34* mRNA expression observed in lesional versus both nonlesional and normal epidermis and with slightly lower dermal mRNA expression (Fig 3, *F*). We also measured *CSF1R* mRNA expression, which was significantly higher in the dermis, regardless of tissue (Fig 3, *G*).

LCM highlights tight junction defects in patients with AD

Because defective barrier function is a hallmark of AD,[1] we evaluated for EDC and cornified envelope (CE) markers. A heat map of EDC and CE genes (including *S100A* genes) is shown in Fig E5 in this article's Online Repository at www.jacionline.org. The majority of S100 genes (*S100A8*/*S100A9*/*S100A12*/*S100A13*), IL-17–induced *PI3*/Elafin, and SPRRs *(SPRR1A)* showed a primarily epidermal expression and higher expression in lesional versus both nonlesional and normal skin (FDR < 0.001 for most markers), whereas a few S100 genes (*S100A4*/*S100A6*/*S100A10*) showed predominantly dermal lesional expression. As previously reported in bulk tissues,[26] the differentiation genes (*LCE*, *LOR*, *FLG*, and periplakin *[PPL]*) showed decreased expression in lesional versus nonlesional and normal epidermis (see Fig E5 and Table E10 in this article's Online Repository at www.jacionline.org). Claudins, another crucial barrier component, are essential for tight junction (TJ) formation. Twenty-three claudins have been identified in human subjects; however, their contribution to AD is not fully defined.[30,31] To gain insight into which claudins are expressed in patients with AD, we evaluated a subset of TJ genes, the expression profiles of which are visualized in a heat map (Fig 4, *A*, and see Table E11 in this article's Online Repository at www.jacionline.org). Downregulation of claudins 1 and 23 was observed in lesional versus nonlesional and normal epidermis, as well as downregulation of claudins 4 and 8, which were previously unreported in patients with AD (FDR < 0.001).[32] We also detected dermal claudins (5 and 11), expression of which was significantly downregulated in the lesional versus normal skin comparison, which was previously not reported in patients with AD.

The differential expression of claudin genes in the epidermal and dermal compartments was validated by using immunohistochemistry and RT-PCR. CLDN4, CLDN8, and CLDN23 stained all epidermal layers, except the stratum corneum (Fig 4, *B-D*), with highly attenuated staining in lesional versus both nonlesional and normal epidermis. The reduced staining was particularly evident in the granular layer. CLDN8 showed increased intensity of basal layer staining in normal epidermis (Fig 4, *C*). The mRNA expression of *CLDN8* and *CLDN23* was also significantly reduced in lesional epidermis ($P < .05$; Fig 4, *E* and *F*).

Markers associated with activated T cells and other inflammatory cells are enriched by using LCM

Using individual cell-culture expression data (keratinocytes, fibroblasts, activated and unactivated T cells, DCs, and LCs),[33-35] we explored the distribution of DEGs identified in epidermal, dermal, and bulk AD transcriptomes[27] using a Gene Set Enrichment Analysis. Whereas only the keratinocyte gene subset was enriched in the epidermal transcriptome (Fig 5 and see Table E12, *A*, in this article's Online Repository at www.jacionline.org), the dermal transcriptome showed enrichment of key inflammatory subsets, including activated and unactivated T cells, various DC subsets (immature and mature DCs), macrophages, fibroblasts, and lymphatic endothelial cells (Fig 5 and see Table E12, *B*). The bulk transcriptome showed a significant enrichment for keratinocytes, fibroblasts, and inflammatory subsets, with no enrichment for activated T cells and mature DCs (Fig 5 and see Table E12, *C*).

The Gene Set Enrichment Analysis also linked key mediators (*IL22*, TNF superfamily, member 4 [*TNFSF4*/OX40L], and *CTLA4*) detected in the dermal transcriptome to the gene signature of activated T cells (see Table E12, *B*). Among the genes found to be associated with both activated and unactivated T cells in the dermal transcriptome were *GZMB*, *ICOS*, and *CD27*.

CCR7, which is associated with T-cell trafficking and cutaneous lymphoid aggregates,[36,37] was shown to be expressed by various cells types, including T cells and DCs. To investigate the predominant cellular expression of CCR7, we performed double immunofluorescence staining for $CD3^+$ T cells (green) or $CD11c^+$ myeloid DCs (green) with CCR7 (red) in lesional, nonlesional, and normal skin. CCR7 colocalized mainly with CD11c, showing increased expression in lesional versus nonlesional and normal dermis and some colocalization with CD3, primarily in lesional dermis (see Fig E6 in this article's Online Repository at www.jacionline.org). Thus CCR7 is preferentially expressed by myeloid DCs rather than T cells.

DISCUSSION

Evolving disease concepts associate the AD phenotype with barrier and immune abnormalities.[1,2] In this model altered proliferation and differentiation of keratinocytes result from

cytokines derived from distinct T-cell subsets.[2,12] It is important to understand the relative contributions of the epidermal and dermal compartments in creating the abnormal lesional phenotype to fully understand the pathogenic mechanisms driving AD.[26]

This is the first report that establishes robust epidermal and dermal genomic signatures of lesional and nonlesional AD and normal skin compared with corresponding whole-tissue fingerprinting. Using bulk skin, we have associated the AD phenotype with T_H2/T_H22 immune activation and abnormal epidermal differentiation.[11-14] However, in bulk genomic profiling we could not determine which compartments are responsible for individual gene expression or locate their cellular sources.[4,12,27] Furthermore, because of a dilution effect in bulk tissues, which are composed of functionally heterogeneous cells, many genes linked to AD pathogenesis are present at less than the detection level on microarrays.[11,12,26,27] Additionally, because a large subset of genes are expressed in either the epidermis or dermis only, some of the measured differential gene expression between lesional and nonlesional skin appears to be an artifact of the unequal contribution of epidermal expansion in lesional skin rather than because of true changes in gene expression at the cellular level. The previous disease model for AD, which has relied on bulk tissue genomic profiling, is limited by the inability to distinguish between these differences. A large proportion of DEGs found only in bulk tissue seem to derive from unequal contributions of lesional epidermis and dermis compared with nonlesional epidermis and dermis. Overall, we believe that the differences in cellular physiology created by AD are best detected in the LCM-generated DEGs.

Using the LCM method followed by genomic and cellular studies, we have identified a largely increased AD transcriptome, with an additional 674 upregulated and 405 downregulated genes compared with prior reports.[11,12,26,27] By separating the 2 compartments, we have also identified key immune and barrier markers that are usually undetectable on arrays (ie, IL-22 and TSLP) and obtained more robust genomic differences for most immune genes when comparing lesional, nonlesional, and normal tissues. Through this approach and previously acquired pathways and cell-specific genomic maps,[11-14,26,27] we have localized many immune and barrier genes to the epidermis or dermis (or both), leading to a deeper understanding of inflammatory circuits and the cellular subset involved in creating the AD phenotype. For example, dermal expression of CCL19 and CCL21 likely attracts $CCR7^+/CD11c^+$ DCs and might organize lymphoid tissue in the dermis. Our LCM and genomic approach also led to enrichment of gene products associated with activated T cells and inflammatory DCs that play a role in effector responses in patients with AD.[37]

Our data are the first to identify IL-34, the newly identified cytokine in mice models, and its receptor, CSF-1R, in a human skin disease. The mouse studies demonstrated a critical role for IL-34 in differentiation and proliferation of LCs in the epidermis during steady states, whereas repopulation of LCs in inflammatory states was independent of IL-34.[28] Although IL-34 is mainly produced by keratinocytes, its receptor, CSF-1R, originates from dermal macrophages and mononuclear cells.[29] Our data show decreased epidermal expression of IL-34 in lesional epidermis compared with that seen in both nonlesional AD and normal epidermis (Fig 3, *B* and *C*). This confirms the role of IL-34 in the maintenance phase, corresponding to prior mouse data.[28] Thus the IL-34 cytokine might function as a negative regulator, and its induction in nonlesional skin might inhibit the propagation of the inflammatory cascade toward development of active skin lesions. Additionally, we found that IL-34 expression in lesional dermis colocalizes most commonly with myeloid DCs and macrophages. Future studies are needed to evaluate the possible functions of the IL-34/CSF-1R cytokine-receptor complex in background and diseased AD skin and whether strategies of increasing levels of this cytokine might be able to prevent development of skin lesions.

Separating the 2 compartments, we also identified 2 novel barrier genes, *CLDN4* and *CLDN8*, for the first time in the AD transcriptome. Claudins are pivotal for TJ formation.[38] Prior mouse and human skin equivalent models demonstrated that CLDN4 colocalized with CLDN1 to the epidermal granular layer,[39,40] whereas CLDN8 was previously shown in human kidneys and intestines.[41,42] Nevertheless, our knowledge of claudins and their involvement in the barrier alterations seen in patients with AD remains incomplete.[29] De Benedetto et al[32] reported that *CLDN1* and *CLDN23* show significantly reduced expression in nonlesional AD skin compared with that seen in healthy skin. In our study *CLDN8* and *CLDN23* showed significantly reduced expression in lesional compared with nonlesional and normal epidermis by using microarrays (Fig 4, *A*, and see Table E11), with respective fainter epidermal staining of CLDN4, CLDN8, and CLDN23 in lesional versus nonlesional AD and normal epidermis (Fig 4, *B* and *D*). Claudin 11 was identified as a novel dermal claudin, which was previously shown in other tissues (brain, testis, and cochlea).[43-45] Future experiments are needed to investigate the function of the newly identified CLDN4 and CLDN8, but together with CLDN1 and CLDN23, these might contribute to the barrier defect associated with the AD phenotype.

Our study also had some limitations. First, LCM is a labor-intensive method, usually allowing analyses of a small number of samples, as in our study (n = 5 lesional and nonlesional specimens each and n = 3 normal samples separated into epidermis and dermis categories), possibly resulting in weaker statistical power, particularly for bulk tissue comparisons. Second, although our LCM approach detected novel barrier genes, the downregulation of key differentiation markers (ie, *FLG*, *LOR*, and involucrin *[IVL]*) in the lesional and nonlesional (vs normal) epidermal transcriptomes was not as impressive as in prior bulk data,[13,26] which is contrary to the enrichment of *FLG* and *LOR* in a prior normal skin epidermis LCM study,[17,46] perhaps because of lower recovery of granular layer products using the epidermal-dermal separation approach.[47] Third, even though the combined LCM epidermal and dermal transcriptomes were larger than the bulk tissue transcriptome, many genes were only detected in the bulk transcriptome (see Fig E2 and Table E8, *C*). This might be explained by (1) the unequal contribution of lesional epidermis and dermis compared with their counterparts; (2) possible inclusion of subcutaneous tissue in bulk biopsy specimens; (3) platform/technical issues, as described in a previous LCM article separating the epidermis and dermis from only 3 psoriatic (lesional and nonlesional) and 3 normal tissues[16]; and (4) restriction of this analysis to patients with severe AD, in whom nonlesional skin has a more abnormal phenotype.[26] Thus many genes might not pass defined thresholds of FCH and significance when comparing lesional and nonlesional skin.

Our study establishes the utility of LCM in patients with AD to separate different skin compartments and cellular infiltrates. It provides complementary information to bulk analysis, allowing regional and/or cellular localization of key barrier or immune molecules, and enables detection of genes that are not usually detected on arrays because of the mixture of transcripts within the heterogeneous bulk tissue.[48,49] LCM is particularly beneficial for AD, in which a complex network of immune and barrier abnormalities results in the global phenotypes of active and "normal-appearing" skin, and dissecting the individual skin components and cells is crucial to unraveling their respective contributions to pathogenesis. Our combined LCM and genomic approach can be useful in future studies aimed at dissecting the relative roles of barrier versus immune activation of different AD phenotypes (ie, intrinsic and extrinsic AD)[11] and for dissecting therapeutic responses to various agents that are now in clinical trials for patients with AD.[50]

Clinical implications: Our approach can be useful to differentiate the ability of targeted treatments to reverse epidermal and immune alterations in AD skin.

REFERENCES

1. Bieber T. Atopic dermatitis. N Engl J Med 2008;358:1483-94.
2. Guttman-Yassky E, Nograles KE, Krueger JG. Contrasting pathogenesis of atopic dermatitis and psoriasis—part I: clinical and pathologic concepts. J Allergy Clin Immunol 2011;127:1110-8.
3. Boguniewicz M, Leung DY. Recent insights into atopic dermatitis and implications for management of infectious complications. J Allergy Clin Immunol 2010;125:4-15.
4. Nograles KE, Zaba LC, Shemer A, Fuentes-Duculan J, Cardinale I, Kikuchi T, et al. IL-22-producing "T22" T cells account for upregulated IL-22 in atopic dermatitis despite reduced IL-17-producing TH17 T cells. J Allergy Clin Immunol 2009;123:1244-52.
5. Ong PY, Leung DY. Immune dysregulation in atopic dermatitis. Curr Allergy Asthma Rep 2006;6:384-9.
6. Hatano Y, Terashi H, Arakawa S, Katagiri K. Interleukin-4 suppresses the enhancement of ceramide synthesis and cutaneous permeability barrier functions induced by tumor necrosis factor-alpha and interferon-gamma in human epidermis. J Invest Dermatol 2005;124:786-92.
7. Elias PM, Hatano Y, Williams ML. Basis for the barrier abnormality in atopic dermatitis: outside-inside-outside pathogenic mechanisms. J Allergy Clin Immunol 2008;121:1337-43.
8. Onoue A, Kabashima K, Kobayashi M, Mori T, Tokura Y. Induction of eosinophil- and Th2-attracting epidermal chemokines and cutaneous late-phase reaction in tape-stripped skin. Exp Dermatol 2009;18:1036-43.
9. Oyoshi MK, Larson RP, Ziegler SF, Geha RS. Mechanical injury polarizes skin dendritic cells to elicit a T(H)2 response by inducing cutaneous thymic stromal lymphopoietin expression. J Allergy Clin Immunol 2010;126:976-84, e1-5.
10. Demehri S, Morimoto M, Holtzman MJ, Kopan R. Skin-derived TSLP triggers progression from epidermal-barrier defects to asthma. PLoS Biol 2009;7:e1000067.
11. Suarez-Farinas M, Dhingra N, Gittler J, Shemer A, Cardinale I, de Guzman Strong C, et al. Intrinsic atopic dermatitis shows similar TH2 and higher TH17 immune activation compared with extrinsic atopic dermatitis. J Allergy Clin Immunol 2013;132:361-70.
12. Gittler JK, Shemer A, Suarez-Farinas M, Fuentes-Duculan J, Gulewicz KJ, Wang CQ, et al. Progressive activation of T(H)2/T(H)22 cytokines and selective epidermal proteins characterizes acute and chronic atopic dermatitis. J Allergy Clin Immunol 2012;130:1344-54.
13. Guttman-Yassky E, Suarez-Farinas M, Chiricozzi A, Nograles KE, Shemer A, Fuentes-Duculan J, et al. Broad defects in epidermal cornification in atopic dermatitis identified through genomic analysis. J Allergy Clin Immunol 2009;124:1235-44.e58.
14. Guttman-Yassky E, Lowes MA, Fuentes-Duculan J, Whynot J, Novitskaya I, Cardinale I, et al. Major differences in inflammatory dendritic cells and their products distinguish atopic dermatitis from psoriasis. J Allergy Clin Immunol 2007;119:1210-7.
15. Espina V, Wulfkuhle JD, Calvert VS, VanMeter A, Zhou W, Coukos G, et al. Laser-capture microdissection. Nat Protoc 2006;1:586-603.
16. Mitsui H, Suarez-Farinas M, Belkin DA, Levenkova N, Fuentes-Duculan J, Coats I, et al. Combined use of laser capture microdissection and cDNA microarray analysis identifies locally expressed disease-related genes in focal regions of psoriasis vulgaris skin lesions. J Invest Dermatol 2012;132:1615-26.
17. Gulati N, Krueger JG, Suarez-Farinas M, Mitsui H. Creation of differentiation-specific genomic maps of human epidermis through laser capture microdissection. J Invest Dermatol 2013;133:2640-2.
18. Ning H, Mitsui H, Wang C, Suarez-Farinas M, Gonazleaz J, Shah K, et al. Identification of anaplastic lymphoma kinase as a potential therapeutic target in basal cell carcinoma. Oncotarget 2013;4:2237-48.
19. Dhingra N, Shemer A, Correa da Rosa J, Rozenblit M, Suarez-Farinas M, Fuentes-Duculan J, et al. Molecular profiling of contact dermatitis skin identifies allergen-dependent differences in immune response. J Allergy Clin Immunol 2014;134:362-72.
20. Gentleman RC, Carey VJ, Bates DM, Bolstad B, Dettling M, Dudoit S, et al. Bioconductor: Open software development for computational biology and bioinformatics. Genome Biol 2004;5:R80.
21. Suarez-Farinas M, Pellegrino M, Wittkowski K, Magnasco M. Harshlight: a "corrective make-up" program for microarray chips. BMC Bioinformatics 2005;6:294.
22. Wu Z, Irizarry RA, Gentleman R, Martinez-Murillo F, Spencer F. A model-based background adjustment for oligonucleotide expression arrays. J Am Stat Assoc 2004;99:909-17.
23. Smyth GK. limma: linear models for microarray data. In Gentleman R, Carey VJ, Huber W, Irizarry RA, Dudoit S, editors. Bioinformatics and computational biology solutions using R and Bioconductor. New York: Springer-Verlag; 2005, pp. 397–420.
24. Boedigheimer MJ, Wolfinger RD, Bass MB, Bushel PR, Chou JW, Cooper M, et al. Sources of variation in baseline gene expression levels from toxicogenomics study control animals across multiple laboratories. BMC Genomics 2008;12:285.
25. Johnson WE, Li C, Rabinovic A. Adjusting batch effects in microarray expression data using empirical bayes methods. Biostatistics 2007;8:118-27.
26. Suarez-Farinas M, Tintle SJ, Shemer A, Chiricozzi A, Nograles K, Cardinale I, et al. Nonlesional atopic dermatitis skin is characterized by broad terminal differentiation defects and variable immune abnormalities. J Allergy Clin Immunol 2011;127:954-64, e1-4.
27. Khattri S, Shemer A, Rozenblit M, Dhingra N, Czarnowicki T, Finney R, et al. Cyclosporine in patients with atopic dermatitis modulates activated inflammatory pathways and reverses epidermal pathology. J Allergy Clin Immunol 2014;133:1626-34.
28. Greter M, Lelios I, Pelczar P, Hoeffel G, Price J, Leboeuf M, et al. Stroma-derived interleukin-34 controls the development and maintenance of Langerhans cells and the maintenance of microglia. Immunity 2012;37:1050-60.
29. Sasmono RT, Oceandy D, Pollard JW, Tong W, Pavli P, Wainwright BJ, et al. A macrophage colony-stimulating factor receptor-green fluorescent protein transgene is expressed throughout the mononuclear phagocyte system of the mouse. Blood 2003;101:1155-63.
30. Tsukita S, Furuse M, Itoh M. Multifunctional strands in tight junctions. Nat Rev Mol Cell Biol 2001;2:285-93.
31. Lal-Nag M, Morin PJ. The claudins. Genome Biol 2009;10:235.
32. De Benedetto A, Rafaels NM, McGirt LY, Ivanov AI, Georas SN, Cheadle C, et al. Tight junction defects in patients with atopic dermatitis. J Allergy Clin Immunol 2011;127:773-86, e1-7.
33. Chiricozzi A, Nograles KE, Johnson-Huang LM, Fuentes-Duculan J, Cardinale I, Bonifacio KM, et al. IL-17 induces an expanded range of downstream genes in reconstituted human epidermis model. PLoS One 2014;9:e90284.
34. Nograles KE, Suarez-Farinas M, Shemer A, Fuentes-Duculan J, Chiricozzi A, Cardinale I, et al. Atopic dermatitis keratinocytes exhibit normal T(H)17 cytokine responses. J Allergy Clin Immunol 2010;125:744-6, e1-746.
35. Fujita H, Nograles KE, Kikuchi T, Gonzalez J, Carucci JA, Krueger JG. Human Langerhans cells induce distinct IL-22-producing CD4+ T cells lacking IL-17 production. Proc Natl Acad Sci U S A 2009;106:21795-800.
36. Forster R, Davalos-Misslitz AC, Rot A. CCR7 and its ligands: balancing immunity and tolerance. Nat Rev Immunol 2008;8:362-71.
37. Guttman-Yassky E, Nograles KE, Krueger JG. Contrasting pathogenesis of atopic dermatitis and psoriasis—part II: immune cell subsets and therapeutic concepts. J Allergy Clin Immunol 2011;127:1420-32.
38. Agrawal R, Woodfolk JA. Skin barrier defects in atopic dermatitis. Curr Allergy Asthma Rep 2014;14:433.
39. Furuse M, Hata M, Furuse K, Yoshida Y, Haratake A, Sugitani Y, et al. Claudin-based tight junctions are crucial for the mammalian epidermal barrier: a lesson from claudin-1-deficient mice. J Cell Biol 2002;156:1099-111.

40. Yuki T, Komiya A, Kusaka A, Kuze T, Sugiyama Y, Inoue S. Impaired tight junctions obstruct stratum corneum formation by altering polar lipid and profilaggrin processing. J Dermatol Sci 2013;69:148-58.
41. Juric M, Xiao F, Amasheh S, May O, Wahl K, Bantel H, et al. Increased epithelial permeability is the primary cause for bicarbonate loss in inflamed murine colon. Inflamm Bowel Dis 2013;19:904-11.
42. Hou J, Renigunta A, Yang J, Waldegger S. Claudin-4 forms paracellular chloride channel in the kidney and requires claudin-8 for tight junction localization. Proc Natl Acad Sci U S A 2010;107:18010-5.
43. Bronstein JM, Micevych PE, Chen K. Oligodendrocyte-specific protein (OSP) is a major component of CNS myelin. J Neurosci Res 1997;50:713-20.
44. Gow A, Southwood CM, Li JS, Pariali M, Riordan GP, Brodie SE, et al. CNS myelin and sertoli cell tight junction strands are absent in Osp/claudin-11 null mice. Cell 1999;99:649-59.
45. Kitajiri SI, Furuse M, Morita K, Saishin-Kiuchi Y, Kido H, Ito J, et al. Expression patterns of claudins, tight junction adhesion molecules, in the inner ear. Hear Res 2004;187:25-34.
46. Kennedy-Crispin M, Billick E, Mitsui H, Gulati N, Fujita H, Gilleaudeau P, et al. Human keratinocytes' response to injury upregulates CCL20 and other genes linking innate and adaptive immunity. J Invest Dermatol 2012;132:105-13.
47. Radoja N, Gazel A, Banno T, Yano S, Blumenberg M. Transcriptional profiling of epidermal differentiation. Physiol Genomics 2006;27:65-78.
48. Liu A. Laser capture microdissection in the tissue biorepository. J Biomol Tech 2010;21:120-5.
49. Decarlo K, Emley A, Dadzie OE, Mahalingam M. Laser capture microdissection: methods and applications. Methods Mol Biol 2011;755:1-15.
50. Guttman-Yassky E, Dhingra N, Leung DY. New era of biologic therapeutics in atopic dermatitis. Expert Opin Biol Ther 2013;13:549-61.

Have you seen the new *JACI* website?

Enjoy these benefits and more:

- Stay current in your field with Featured Articles of The Week, Articles in Press, and easily view the Most Read and Most Cited articles.
- Sign up for a personalized alerting service with Table of Contents Alerts, Articles in Press Alerts and Saved Search Alerts to be notified when new articles relevant to you are available.
- Create your own Reading List for future reference.
- Link from cited references to abstracts and full text of other participating journals.
- Access additional features such as audio podcasts and the *JACI* Journal Club Blog.

Visit www.jacionline.org today to see what else is new online!

Methods

Skin samples

Pre-treatment paired non-lesional/NL and lesional/LS AD skin biopsies were collected from 5 patients with moderate-to-severe chronic atopic dermatitis (3 males and 2 females, age: 27-59 years; mean age: 39.4 years) (ETable1) under a protocol approved by The Rockefeller University's Institutional Review Board. Serum IgE levels (reference range: 0-160 kU/L) were increased in 2 of 5 patients (range: 14-1821 kU/L; mean: 495.4 kU/L) and serum eosinophil counts (reference range: 0% to 7%) were increased in 3 of 5 patients. The Scoring of AD (SCORAD) index ranged from 45 to 65 (mean: 56.8). Normal skin samples from healthy volunteers, previously collected for a prior LCM publication,[E1] were also included for comparisons with AD skin (this in-house study consisted of epidermal, dermal, and bulk samples, with only epidermal samples presented in the publication). Microarray data were collected from LS and NL epidermal, dermal, and full thickness samples (n=5). Comparison of LS and NL microarray expression values was made with 10 epidermal, 6 dermal, and 6 bulk corresponding normal samples. For RT-PCR confirmation, 3 normal paired epidermis and dermis samples were used, due to the limited amount of available mRNA. Due to the labor-intensive and time-consuming nature of the method, we present a relatively small sample size. However, separating the skin compartments into dermis and epidermis has been shown to provide a gain in sensitivity, overcoming the limitations introduced by the sample size. Furthermore, the paired nature of the data reduces the number of confounding

factors and thereby increases the sensitivity.

Slide preparation and Laser Capture Micro-dissection/LCM

Frozen AD skin samples were cut into 8.0μm sections in a -20°C cryostat. An abbreviated Hematoxylin & Eosin (H&E) staining technique was used in preparation for LCM. LCM was performed following the manufacturer's protocol for CellCut system (Molecular Machines & Industries, Haslett, MI) and epidermal and dermal regions were dissected from each sample as shown in Fig.1A. In detail, we regarded dermis as combined papillary and reticular dermis and dermal inflammatory cell infiltration. Dissected samples were placed in 100μL of RLT buffer (Qiagen, Valencia, CA) containing 1% beta - mercaptoethanol (Fisher Scientific, Hampton, NH) within 2 hours of the initial staining step in order to minimize RNA degradation.

RNA extraction and quantification of LCM cells

Total RNA was extracted using RNeasy Micro Kit (Qiagen, Valencia, CA) according to the manufacturer's protocol with on-column DNase digestion. The amount of RNA was assessed by quantitative RT-PCR using EZ PCR Core Reagents (Applied Biosystems, Foster City, CA) for the human acidic ribosomal protein (hARP) housekeeping gene (primer sequences were listed in ETable2), using the 7900HT Fast Real-Time PCR System (Applied Biosystems), with the following thermal cycler conditions: 2 minutes at 50°C; 30 minutes at 60°C; 5 minutes at 95°C; then 45 cycles of 15 seconds at 95°C followed by 60 seconds at 62°C. Assays were performed in triplicate.

Sample preparation for gene chip analysis

We used Human Genome U133 Plus 2.0 GeneChip probe arrays (Affymetrix, Inc) containing approximately 54,000 probe sets to assess expression of more than 47,000 transcripts, including approximately 38,500 genes and unigenes. Total RNA (10ng) was subjected to a two-cycle cDNA synthesis method, as previously reported.[E2] Labeling ofEcRNA transcripts with biotin was performed by BioArray HighYield RNA transcript labeling kit (Enzo Biochem). 15μg of the biotinylated cRNA was fragmented and hybridized to HGU133 plus 2.0 arrays. The chips were washed, stained with streptavidin-phycoerythrin, and scanned according to the manufacturer's protocol.

Sample preparation for quantitative real-time PCR (RT-PCR)

Reverse transcription to cDNA from RNA of LCM samples was carried out using the High Capacity cDNA Reverse Transcription kit (Applied Biosystems) according to the manufacturer's instructions. 1ng of total RNA was mixed with 20μl of cDNA synthesis reaction containing 1μl of RNase inhibitor. 12.5μl of the resulting cDNA was then amplified using TaqMan® PreAmp Master Mix (Applied Biosystems). The 50μl preamplification PCR reaction included 25 μl of 2× TaqMan® PreAmp Master Mix and 12.5μl of pooled assay mix prepared by combining 20× TaqMan® Gene Expression Assays into a single tube and using 1× TE buffer to dilute the pooled assays to a final concentration of 0.2×. The reactions were incubated at 95°C for 10 min, followed by 14 cycles of 95°C for 15 sec and 60°C for 4 min. The preamplified cDNA product was 1:20 diluted and analyzed using TaqMan® Gene Expression Master Mix following the

manufacturer's procedures. The RT-PCRs for each assay were run in triplicate.

Immunohistochemistry (IHC)

LS, NL, and N frozen sections were prepared from biopsies. The slides were stained with IL-34, and Claudins 4, 8, and 23. Tissue sections were incubated with primary antibodies at 4°C overnight. Secondary biotin-labeled horse anti-mouse antibody or goat anti-rabbit antibody (Vector Laboratories, Burlingame, CA) was amplified with avidin-biotin complex (Vector Laboratories). 3-Amino-9-ethylcarbazole (Sigma-Aldrich, St. Louis, MO) was the chromogen used. Primary antibodies and their dilutions used are listed in ETable3.

Immunofluorescent staining (IF)

Frozen sections of LS, NL, and N skin were prepared. The slides were fixed with acetone and blocked in 10% normal goat serum (Vector Laboratories) for 30 minutes. Primary antibodies for CCR7 or IL-34 were incubated overnight at 4°C and amplified with the appropriate secondary antibody. For co-localization with CD3, CD11c and CD163, sections were then co-stained overnight with a second primary antibody and amplified with the appropriate secondary antibody for 30 minutes. Antibodies and their dilutions used are listed in ETable3.

Statistical Analysis

All statistical analysis of the microarray data and the RT-PCR data was carried out using *R* and *Bioconductor* packages.[E3] We used the *Harshlight* package to automatically detect and adjust for extended, diffuse, and compact blemishes on the microarray chips. Analysis of RT-PCR data ($\log_2$ scale of the normalized value) was carried out using a linear mixed model with

tissue/compartment as a fixed effect and patient as a random effect. Initial summarization, normalization and assessment of the raw expression values was carried out using the *GCRMA algorithm (Bioconductor GCRMA* package),[E4] accounting for the individual probes' affinity towards non-specific binding by utilizing specific probe sequence information. *GCRMA* converts the adjusted probe intensities of the microarray chips to expression values applying the *rma* (Robust Multiarray Average) normalization and summarization methods, taking into account sequence information of the individual probes to estimate their affinities to non-specific binding (NSB). Generally, principal component analysis/PCA was applied to summarize the microarray expression profiles from the multi-dimensional to a two-dimensional space. Batch effects between samples run on different days were assessed by principal component analysis and principal variant component analysis/*PVCA*, and adjusted for by the empirical bayes method *ComBat* implemented in the *Bioconductor* package *SVA*.[E6-8] *ComBat* makes use of an empirical Bayes method framework to adjust for known batches. As bulk tissue and LCM expression data were obtained at different times, PCA showed a clear batch effect between the two datasets, which was readily removed by the empirical bayes method *ComBat*, as indicated by after adjustment PCA plot in Fig.1B. In order to validate the batch effect adjustment, the above procedure was performed using a previously published psoriasis/PSO LCM/bulk dataset (GSE26866) and psoriasis LCM data process in the same batch as the AD LCM data under consideration.

In this comparison, the PSO and AD datasets were preprocessed and normalized jointly. This was followed by a two step batch adjustment, in which firstly, all PSO and AD LCM data were treated as one batch and the AD bulk data as another, and then after, all previous PSO (GSE26866) data were treated as one batch and all AD and corresponding new PSO LCM data as another.

EFig7.A shows the PCA of the combined PSO and AD expression data before adjustments, while EFig.7B-C show the first and second adjustment steps, respectively, indicating a proper adjustment for batch effect between bulk and LCM samples in our AD dataset. Furthermore, assessment of the detected DEGs for the bulk tissue comparisons showed ranges of the top and bottom DEGs that are in line with previously published work.

Model estimation and hypothesis testing for the comparisons of interest were carried out by the mixed-effect framework of the *Bioconductor limma* package,[E9] with patients as a random effect and tissue/compartment as a fixed effect, where the correlation structure used by *limma* is a compound symmetric. *Limma* is a package for performing expression analysis of microarray data in applying linear models to discover differential expression between two groups of samples. P-values were adjusted for multiple testing using the *Benmjamini-Hochberg procedure*,[E10] and genes with a false discovery rate/FDR<0.05 and a fold changeFCH>2.0 were reported as differentially expressed genes/DEGs.

As bulk tissue and LCM expression data were obtained at different times, PCA showed a clear batch effect between these two datasets, which was readily removed by the empirical bayes method *ComBat*, as indicated by the PCA plot in

Fig.1B. In order to validate the batch effect adjustment, the above procedure was performed including a previously published psoriasis LCM dataset, in which the bulk and LCM tissues were processed in the same batch (EFig.7A-C). This comparison indicated a proper adjustment for batch effect between bulk and LCM samples in our AD dataset. Furthermore, assessment of the detected DEGs for the bulk tissue comparisons showed the ranges of the top and bottom DEGs to be in line with previously published work.

Enrichment analysis of genes linked to specific cell types (cell maps – *Mayte Suárez-Fariñas,* personal communication*,* March *2014*) was carried out by Fisher's exact test, with p-value adjustment by the *Benjamini–Hochberg* procedure, applying an adjusted p-value cut-off of 0.05.

Heatmaps were produced by hierarchical clustering with the McQuitty agglomeration method, using the pairwise Pearson correlation distance (1-cor) between the rows of the combined expression set.

Results

Within the bulk tissue transcriptome there was a subset of DEGs that was not identified in the corresponding epidermal and dermal transcriptomes (747 DEGs in total). A heatmap of the 747 genes is shown in EFig.3A. Analyzing these DEGs revealed that 70% (534 DEGs) show significant differential expression in normal epidermis vs. dermis. This suggests that the measured bulk tissue differential expression is impacted by the greater contributions of epidermal expression (in LS skin) and greater contributions of dermal expression (in NL skin), since these DEGs are also significant in the normal epidermal vs. dermal comparison (EFig.3B). Of the remaining 223 DEGs not found in the normal tissue epidermal vs. dermal comparison, 77 DEGs (10.3% of total) were also found in epidermal vs. dermal comparisons of the LS and NL skin tissue. 47 of the remaining 146 DEGs (6.3% of total) not found in any epidermal vs. dermal comparison could be attributed to failing to meet the stringent p-value adjustment method (FDR), with FCHs above 2 or below -2, while retaining significant unadjusted p-values. In order to determine the relative contributions of epidermis and dermis, we applied the following multiple linear model to the 747 DEGs unique to bulk tissue, modeling the expression values of these genes in NL and LS skin with proportional epidermal and dermal expression values:

$$Y_{FT,i} = \beta_1 X_{Epi,i} + \beta_2 X_{Derm,i} + \epsilon_i$$

, for gene i (with i = 1,…, 747), where $Y_{FT,i}$ corresponds to the respective full thickness/bulk expression value, β to the regression coefficient (with the restrictions $\beta > 0$ and $\beta_1 + \beta_2 = 1$), $X_{Epi,i}$ and $X_{Derm,i}$ to the average epidermal

and dermal expression values, respectively, and ϵ_i to the normally distributed error term.

This approach resulted in two models, one for each bulk LS and NL:

$$LS_{FT} = 0.64LS_{Epi} + 0.36LS_{Derm}$$

$$NL_{FT} = 0.38NL_{Epi} + 0.62NL_{Derm}$$

, estimating 64% epidermal and 36% dermal contributions to LS expression values, and 38% epidermal and 62% dermal contributions to NL expression values (EFig.3C). These rough model findings are in line with the known epidermal thickening in lesional AD.

Furthermore these models estimate an inflated number of DEGs unique to bulk tissue due to weighted contributions of compartment-specific DEGs, in the special case where $LS \cong NL$ for both the respective epidermal and dermal expression values. The FT/bulk LS vs. NL comparison might appear differentially expressed if the epidermal and dermal log2-expression values differ by 3.84. Similar to epidermis/dermis $LS \cong NL$, bulk LS vs. NL can be written in terms of the above models:

$$LS_{FT} - NL_{FT} = 0.26Epi - 0.26Derm$$

$$\Rightarrow 0.26(Epi - Derm) > 1$$

$$Epi - Derm > 3.84$$

, at the given threshold (log2-FCH $\geq$ 1), where Epi and Derm refer to the respective average expression values, being simplified due to the restriction $LS \cong NL$. An example of this on the expression values for the gene *CFH* is

shown:

$$LS_{FT} = 0.64 * 3.942 + 0.36 * 12.912 = 7.171 \ (actual\ LS_{FT} = 7.166)$$

$$NL_{FT} = 0.38 * 3.779 + 0.62 * 13.943 = 10.081 \ (actual\ NL_{FT} = 10.199)$$

$$LS_{FT} - NL_{FT} = 7.171 - 10.081 = -2.91$$

So, in this example, the levels of contribution to the combined expression value from epidermis and dermis differ from LS (7.171) to NL (10.081), resulting in the observed difference between LS and NL in bulk tissue. If each compartment contributed equally to the expression values in each tissue type, the bulk LS and NL expression values would be in the same range (8.427 and 8.861 respectively).

References

1. Ning H, Mitsui H, Wang C, Suarez-Farinas M, Gonazleaz J, Shah K, et al. Identification of anaplastic lymphoma kinase as a potential therapeutic target in Basal Cell Carcinoma. Oncotarget. 2013; 4(12): 2237–2248.
2. Mitsui H, Suarez-Farinas M, Belkin DA, Levenkova N, Fuentes-Duculan J, Coats I*,* et al. Combined use of laser capture microdissection and cDNA microarray analysis identifies locally expressed disease-related genes in focal regions of psoriasis vulgaris skin lesions. J Invest Dermatol. 2012;132(6):1615-26.
3. Gentleman RC, Carey VJ, Bates DM, Bolstad B, Dettling M, Dudoit S*, et al*. Bioconductor: Open software development for computational biology and bioinformatics. Genome Biol. 2004;5(10):R80.
4. Wu Z, Irizarry RA, Gentleman R, Martinez-Murillo F, Spencer F. A Model-Based Background Adjustment for Oligonucleotide Expression Arrays. Journal of the American Statistical Association, 2004;99(468):909–17.
5. Boedigheimer MJ, Wolfinger RD, Bass MB, Bushel PR, Chou JW, Cooper M, et al. Sources of variation in baseline gene expression levels from toxicogenomics study control animals across multiple laboratories. BMC Genomics. 2008;12(9):285.
6. Chen C, Grennan K, Badner J, Zhang D, Gershon E, Jin L, et al. Removing batch effects in analysis of expression microarray data: An evaluation of six batch adjustment methods. PLoS One. 2011;28;6(2):e17238.

7. Johnson WE, Li C, Rabinovic A. Adjusting batch effects in microarray expression data using empirical Bayes methods. Biostatistics (Oxford, England) 2007;8(1):118–27.
8. Johnson WE, Li C, Rabinovic A. Adjusting batch effects in microarray expression data using empirical bayes methods. Biostatistics. 2007;8(1):118-27.
9. Smyth GK. limma: Linear Models for Microarray Data. In R. Gentleman, V. J. Carey, W. Huber, R. A. Irizarry, & S. Dudoit (Eds.), Bioinformatics and Computational Biology Solutions Using R and Bioconductor (V., pp. 397–420). New York: Springer-Verlag.
10. Benjamini Y, Hochberg Y. Controlling the false discovery rate: a practical and powerful approach to multiple testing. Journal of the Royal Statistical Society, 1995;57(1):289–300.

Supplementary Figure Legends

EFigure 1. Unsupervised hierarchical clustering of expression values of genes differentially expressed between normal epidermis and dermis, shown across lesional/LS; non-lesional/NL and normal/N skin in bulk, epidermis or dermis. (n=5 for AD; n=6, 10, and 6 for normal bulk, epidermis, and dermis, respectively)

EFigure 2. A Venn diagram of the LCM epidermis and dermis and bulk AD transcriptome comparing LS and NL (fold change/FCH>2.0, false discovery rate/FDR<0.05, green/upregulated; red/downregulated).

EFigure 3. A. A heatmap of differentially expressed genes/DEGs uniquely identified in bulk tissue. **B.** A Venn diagram highlighting the number of unique DEGs identified in bulk tissue, with the numbers of genes in the following subsets: genes identified in the comparison of normal epidermis vs. dermis **(i)**, genes identified in the comparison of LS and NL epidermis vs. dermis **(ii)**, genes that miss the strict FDR threshold/FDR<0.05, but retain significant unadjusted p-values **(iii)**, and genes not identified in **i-iii (iv) C.** Schematic of LS and NL skin showing relative contributions of each compartment as estimated by the linear model.

EFigure 4. Representative immunofluorescence staining for co-expression of IL-34 (red) and $CD3^+$ T-cells (green) **(A),** $CD11c^+$ DCs **(B)** and $CD163^+$

macrophages (green) **(C)** in lesional/LS and non-lesional/NL AD and normal/N skin.

EFigure 5. A heatmap of epidermal differentiation complex/EDC and the cornified envelope/CE genes, showing FCH differences comparing LS; NL and N skin in bulk; epidermis or dermis. (n=5 for AD; n=6, 10, and 6 for normal bulk, epidermis, and dermis, respectively)

EFigure 6. Representative immunofluorescence staining for co-expression of CCR7 (red) and $CD3^+$ T-cells (green) **(A)** and CCR7 (red) and $CD11c^+$ DCs (green) **(B)** in lesional/LS and non-lesional/NL AD and normal/N skin. White arrows indicate double-positive cells.

EFigure 7. Principal component analysis/PCA plots of combined AD and PSO (previously published and this study) LCM/bulk data before **(A),** and after, adjusting for batch effects with batch “AD-bulk” **(B),** and with batch “Researcher” **(C).**

ETable 1. Characteristics of AD patients.

ETable 2. Primers and probes used for RT-PCR.h

ETable 3. Antibodies used for IHC and IF.

ETable 4. Top 25 up- **(A)** and down-regulated **(B)** differentially expressed genes in AD non-lesional/NL dermis versus non-lesional/NL epidermis.

ETable 5 Top 25 up- **(A)** and down-regulated **(B)** differentially expressed genes in AD lesional/LS dermis versus lesional/LS epidermis.

ETable 6 Top 25 differentially expressed genes up-regulated in the epidermis **(A)** and dermis **(B)** differentially expressed genes in AD lesional/LS versus non-lesional/NL skin.

ETable 7 Top 25 differentially expressed genes down-regulated in the epidermis **(A)** and dermis **(B)** in AD lesional/LS versus non-lesional/NL skin.

ETable 8. Full table of all differentially expressed genes (FCH<2.0 and FDR<0.05) in the unique LCM epidermal **(A)**, unique LCM dermal **(B)**, unique bulk **(C)**, and non-unique **(D)** transcriptomes, including all comparisons between lesional/LS, non-lesional/NL, and normal epidermis, dermis, and bulk tissues.

ETable 9. All comparisons of gene expression values in the immune-related gene subset shown in Fig.2A. Status 1 is differentially expressed, 0 is not differentially expressed.

ETable 10. All comparisons of gene expression values in the epidermal differentiation complex/EDC and the cornified envelope/CE gene subset shown in EFig.5. Status 1 is differentially expressed, 0 is not differentially expressed.

ETable 11. All comparisons of gene expression values in the barrier-related gene subset shown in Fig.4A. Status 1 is differentially expressed, 0 is not differentially expressed.

ETable 12. The genes differentially expressed in the bulk (a) and the LCM epidermal (b) and dermal (c) transcriptomes comparing lesional/LS and non-lesional/NL with possible cellular source. (KC/keratinocyte, iDC/immature dendritic cell, LEC/lymphatic endothelial cell, MVEC/microvascular endothelial cell, mDC/mature dendritic cell).